



Reliability Analysis of Boost Converters Connected to a Solar Panel Using a Markov Approach

Rifqi Firmansyah Muktiadji¹ and Ali Muhammad Rushdi^{1*}

¹*Department of Electrical and Computer Engineering, King Abdulaziz University, Jeddah 21589, Saudi Arabia.*

Authors' contributions

This work was carried out in collaboration between the two authors. Author RFM performed the analysis, solved the detailed example, wrote the first draft of the main text of the manuscript and initiated the literature search. Author AMR envisioned and designed the study, contributed to the symbolic and numerical analysis, checked the solution of the detailed example, managed and finalized the literature search, wrote the appendix and substantially edited and improved the entire manuscript. Both authors read and approved the final manuscript.

Article Information

DOI: 10.9734/JENRR/2021/v7i130182

Editor(s):

(1) Dr. Huan-Liang Tsai, Da-Yeh University, Taiwan.

Reviewers:

(1) Doston Khasanov Turayevich, Tashkent University of Information Technologies named after Muhammad al-Khwarizmi (TUIT), Uzbekistan.

(2) R. Sujatha, SSN College of Engineering, India.

Complete Peer review History: <http://www.sdiarticle4.com/review-history/64839>

Original Research Article

Received 10 November 2020

Accepted 16 January 2021

Published 05 February 2021

ABSTRACT

In the past few decades, the energy shortage and global warming problems became a serious concern for humanity. To solve these problems, many countries have evolved renewable energy sources (RESs) such as solar, wind, hydro, tidal, geothermal, and biomass energy sources. Solar energy is usually harvested via a solar panel that is connected to a boost converter to supply the loads. The converter has a key role in the system, since it controls the voltage at the DC bus. If any accidental fault occurs in the converter, the solar panel cannot supply electricity to the loads. Therefore, reliability evaluation of the converter is usually warranted. In this study, reliability evaluation of boost converters connected to a solar panel is carried out using the Markov technique. This technique is widely employed to evaluate the reliability and availability of a system with fixed failure and repair rates. Using the Markov method, we found that the reliability of the typical specific converter considered is 0.9986 for $t = 1000$ hours and that its life expectancy or Mean-Time-To-Failure (MTTF) is 713247 hours.

*Corresponding author: E-mail: arushdi@kau.edu.sa;

Keywords: Reliability; boost converters; Markov technique; solar panel.

1. INTRODUCTION

In the past few decades, the energy shortage and the global warming problems became a serious concern for all countries in the world. To solve these problems, many countries have evolved renewable energy sources (RESs) such as solar panels that generate electrical energy in DC form to replace conventional power generation. In order to supply loads such as digital devices and lighting systems, a solar panel should be connected to a DC/DC boost converter [1-3].

The boost converter has an important role in the system, namely, it is responsible for control of the voltage at the DC bus, which is necessary to mitigate any variation that takes place in the solar radiation input of the solar panel. If any accidental fault in the converter happens, the solar panel ceases to supply electricity to the loads. Therefore, evaluation of the reliability of the converter is needed to estimate its expected lifetime and this evaluation is an essential element of any adequate maintenance plan, since it is used for predicting the failure of any component of the converter and for proposing its replace/repair before its actual failure [4–7].

There have been several studies on the reliability analysis of a DC/DC boost converter in the literature [8, 9]. Arifujjaman [8] presented a reliability analysis of power-electronic converters for a grid that is connected to a permanent magnetic synchronous generator (PMSG) wind turbine. The reliability analysis in [9] has been carried out for a push-pull converter which is built to connect to a 125-W solar panel. Failure rates of a solar panel, capacitors and inverters utilized in a grid connected solar power system have been reported in [10].

We use this paper to present reliability analysis of boost converters connected to a solar panel using Markov modeling, which is a powerful technique used for reliability analysis of complex systems that undergo transitions among distinct states, and it is very useful in many practical situations such as smart microgrid energy management systems [11,12], solar farm generation [13], safety systems [14], and large systems [15-18]. Furthermore, the technique is widely employed to carry out reliability and availability evaluation of systems with fixed failure and repair rates [19].

The rest of this paper is structured as follows. The impact of parameters on the pertinent failure

rates is outlined in Section 2. Section 3 describes the method used to evaluate the reliability of the boost converter, namely a method employing a continuous-time discrete-state Markov chain [12-23]. Section 4 discusses reliability analysis of the boost converter. Section 5 concludes the paper. Appendix A outlines methods for analyzing a general two-state Markov chain.

2. PARAMETERS INFLUENCING THE FAILURE RATES OF COMPONENTS OF A BOOST CONVERTER

A boost converter (step-up converter) is a DC-to-DC power converter that boosts (steps up) voltage (while stepping down current). It might be classified as a switched-mode power supply (SMPS) containing at least two semiconductor devices (a diode and a transistor such as a MOSFET) and at least one non-dissipative energy-storage circuit element such as an inductor or a capacitor. In this section, several parameters that have impact on failure rates of each part in the boost converter are discussed. The boost converter considered herein comprises the following specific components: an inductor, a MOSFET, and a diode, as shown in Fig. 1 [23]. The expression of the failure rate for a component part or micro device can be formulated as in (1).

$$\lambda_{part} = \lambda_b \prod_{i=1}^n \pi_i \quad (1)$$

Where n describes the number of the total effective dimensionless factors π_i affecting the failure rate of the specific part of the device. The failure rate for each part or component of the DC/DC boost converter device involves several factors specified as shown in Table 1.

We now digress a little bit to explain the notation in Table 1, wherein λ_L is the inductor failure rate, λ_{sw} is the switch/transistor failure rate, λ_D is the diode failure rate considering both faults of short circuit (SC) and open circuit (OC) and λ_b is a basic failure rate. Moreover, the failure rate of each component is seen to be influenced by several factors such as the quality π_Q , type of the component π_C , the application of device π_A in the system, the environment π_E and the stress of electricity applied on the component π_{ES} . Furthermore, the impact of temperature π_T on the failure rate λ can be specified as shown in Table 2 [24].

Power dissipation impacts the temperature of every part of the system. All aspects (except that of the temperature impact) are presumed to be constant. Equation (2)-(5) report thermal analysis of the system components. Utilizing Ref. [25], we calculate the junction temperature of the component as follows in (2).

$$T_j = T_c + \theta_{jC} P_D \quad (2)$$

where θ_{jC} describes the junction-to-case thermal resistance (Kelvin per watt or K/W), T_j states the junction temperature, while the power dissipation is depicted as P_D and the case temperature T_c is formulated as follows

$$T_c = T_a + \theta_{cA} P_D \quad (3)$$

where, T_a denotes the ambient temperature and θ_{cA} denotes the thermal resistance between the junction and the case. Moreover, the inductor hotspot temperature represented by T_{HS} is a function of its power dissipation P_D and the radiation of the surface area A of the case. According to [25], we can get the following equations

$$T_{HS} = T_a + 1.1 \Delta T \quad (4)$$

$$\Delta T = 1.25 \frac{P_D}{A} \quad (5)$$

The constant 1.25 in (5) is a dimensional (rather than dimensionless) constant. It has units of kelvin times meter squared per watt. The expressions of the power loss for some components of the boost converter are presented in Table 3 [26].

3. DEVELOPMENT OF A MARKOV RELIABILITY MODEL FOR THE DC/DC BOOST CONVERTER

In the literature, the Markov technique is an important method used to evaluate the reliability of complex systems [27]. The Markov technique generally deals with several possible discrete states of the system, rate parameters of the transition paths as well as possible transition paths among the states [21, 27-30]. Fig. 3 shows a trivially simple discrete-state continuous-time Markov chain that models a DC/DC boost converter connected to a solar panel. Fig. 3 is a no-repair special case of Fig. A1 discussed in appendix A. The Markov chain in Fig. 3 is the simplest possible such a chain, with just two states and a single transition. It has a good (up or healthy) state and a failure (down) state. The

failure state represents catastrophic failure and is an absorbing state.

In this study, the reliability of DC/DC boost converters connected to PV panels as shown in Fig. 2 is evaluated by using the Markov method. In Fig. 3, the transition diagram of the converter consists of two states that are a failure state and an initial/healthy/success state. Note that the only failure state is an absorbing state, and hence it stands for catastrophic failure. Fig. 3 is subject to the realistic assumption that the system is without repair, an assumption that we held in the main text but that we relax in Appendix A. The reliability of the converter is its probability of being in the success state, and hence it is expressed as in (6)

$$R(t) = P_1(t) \quad (6)$$

with $P_1(t)$ denoting the healthy state probability. Its governing equation is formulated as in (7) (a special case of the results in Appendix A)

$$\frac{d}{dt} \begin{bmatrix} P_1(t) & P_2(t) \end{bmatrix} = \begin{bmatrix} P_1(t) & P_2(t) \end{bmatrix} \begin{bmatrix} -\lambda_{12} & \lambda_{12} \\ 0 & 0 \end{bmatrix} \quad (7)$$

where, λ_{12} denotes the failure rate of the DC/DC boost converter, which is the transition rate from the healthy state to the absorbing/failure state. We consider the initial state as the healthy state, so that the initial condition of the ordinary differential equation (ODE) (7) can be formulated as

$$\begin{bmatrix} P_1(t) & P_2(t) \end{bmatrix} = \begin{bmatrix} 1 & 0 \end{bmatrix} \quad (8)$$

Equations (7) and (8) constitute a well-formed initial value problem (IVP), whose solution $P_1(t)$ is calculated for non-negative time as

$$P_1(t) = e^{-\lambda_{12}t} \quad (9)$$

A short circuit (SC), an open circuit (OC) and other types of faults of the equipment will cause the total failure of the converter and lead to its permanent switching from the healthy state to the catastrophic-failure state. The overall failure rate λ_{12} is formulated as follows

$$\lambda_{12} = \lambda_L + \lambda_{SW} + \lambda_D \quad (10)$$

Equation (10) is obtained via the assumption that the converter is logically (albeit not physically) a series connection of its three components (inductor, switch, and diode). The factors of quality, voltage stress, environmental influences,

temperature, and power loss that are proposed and formulated in the MIL-HDBK-217 Handbook [6] will definitely impact the failure rate of each component. In (10), the component failure rates are calculated as constant (non time-varying), which is appropriate when each component is operated in the prime-of-life region of the bath-tub curve [31-35]. Note that the bath-tub curve representing the failure rate (hazard rate) versus time consists of three operation intervals namely; (a) the debugging (burn-in, or infant mortality) interval, (b) the prime-of-life (useful life) interval, and (c) the wear-out interval. These three intervals in the bath-tub curve correspond to a decreasing failure rate (DFR), a constant failure rate (CFR), and an increasing failure rate (IFR), respectively [31-35]. We assume that the components of the converter are operating in their useful-life (CFR) intervals, a satisfactory assumption in many real life applications [10]. Finally, the life expectancy or MTTF is described as follows [19, 32, 36-38]

$$MTTF = \int_{t=0}^{\infty} P_1(t)dt = \frac{1}{\lambda_{12}} \quad (11)$$

4. RELIABILITY EVALUATION OF THE DC/DC BOOST CONVERTER

Reliability evaluation of the DC/DC boost converter is obtained by using the Markov method in Equations (6)-(9) and the data of the military handbook MIL-HDBK-217F [6]. The junction temperature T_j of the MOSFET transistor can be calculated using (2) with an assumed ambient temperature $T_a = 25^\circ\text{C}$, a junction-to-case thermal resistance of $\theta_{CA} = 18^\circ\text{C}/\text{W} = 18\text{K}/\text{W}$ and a power dissipation in the MOSFET of $P_{SW} = 1.84\text{ W}$. Finally, we obtain $T_j = 25 + (18 \times 1.84) = 58.17^\circ\text{C}$

Using Table 2, we can obtain the temperature factor of the MOSFET as follows

$$\pi_T = e^{-1925\left(\frac{1}{58.17+273} - \frac{1}{298}\right)} = 1.78$$

Therefore, using Table 1 with $\lambda_b = 0.012$ failure/million hours [6] $\pi_A = 8$, $\pi_Q = 8$, $\pi_E = 1$, we can calculate the failure rate of the MOSFET as follows

$$\lambda_{SW} = \lambda_b \pi_T \pi_A \pi_Q \pi_E = (0.012)(1.78)(8)(8)(1) = 1.37 \text{ failure/million hours.}$$

Similar calculations can be carried out for the failure rates of the diode and the inductor.

Utilizing Table 2, we can get the temperature factor of the diode as follows

$$\pi_T = e^{-3091\left(\frac{1}{T_j+273} - \frac{1}{298}\right)} = 6,$$

and hence, using Table 1 with $\lambda_b = 0.0038$ failure/million hours, $\pi_C = 2$, $\pi_Q = 1$, $\pi_{ES} = 0.09$ $\pi_E = 1$, we can calculate the failure rate of the diode as follows

$$\lambda_D = \lambda_b \pi_T \pi_{ES} \pi_C \pi_Q \pi_E = (0.0038)(6)(0.09)(2)(1)(1) = 0.032 \text{ failure/million hours.}$$

For the failure rate of the inductor, we use Table 2 to obtain the temperature factor of the inductor as follows

$$\pi_T = e^{\frac{-0.11}{8.617 \times 10^{-5}}\left(\frac{1}{T_j+273} - \frac{1}{298}\right)} = 1.29$$

hence, using Table 1 with $\lambda_b = 3 \times 10^{-5}$ failure/million hours, $\pi_Q = 1$, $\pi_E = 1$ and $\pi_C = 2$, we can calculate the failure rate of the diode as follows

$$\lambda_L = \lambda_b \pi_T \pi_Q \pi_E = (3 \times 10^{-5})(1.29)(1)(1) = 0.0000387 \text{ failure/million hours.}$$

The Total failure rate for the DC/DC boost converter can be calculated using (10), and we will get

$$\lambda_{12} = \lambda_L + \lambda_{SW} + \lambda_D = 0.0000387 + 0.032 + 1.37 = 1.4020387 \text{ failure/million hours.}$$

The reliability of the converter can be obtained by using (9) as

$$R(t) = e^{-\lambda_{12}t} = e^{-1.4020387t}$$

where t is measured in million hours. For $t = 1000$ hours = 0.001 million hours, the reliability of the converter is 0.9986. Finally, the MTTF can be calculated by (11) and we obtain it as follows

$$MTTF = \frac{1}{\lambda_{12}} = \frac{1}{1.4020387 \text{ failure/million hours}} = 713247 \text{ hours}$$

Fig. 4 shows the reliability curve of the converter relaxation curve), which represents the plotted against time. The curve in Fig. 4 is a Complementary Cumulative Distribution Function (CCDF) of the exponential distribution [21, 32].

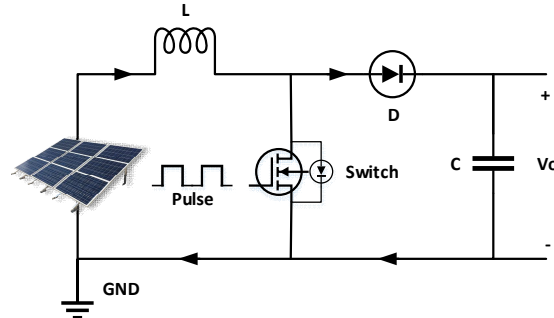


Fig. 1. A DC/DC Boost Converter Connected to a Solar Panel

Table 1. Failure rate models

Component	Failure rate models
Inductor	$\lambda_L = \lambda_b \pi_T \pi_Q \pi_E$
MOSFET	$\lambda_{SW} = \lambda_b \pi_T \pi_A \pi_Q \pi_E$
Diode	$\lambda_D = \lambda_b \pi_T \pi_{ES} \pi_C \pi_Q \pi_E$

Table 2. Temperature factors

Component	Temperature factors
Inductor	$\pi_T = e^{\frac{-0.11}{8.617 \times 10^{-5}} \left(\frac{1}{T_J + 273} - \frac{1}{298} \right)}$
MOSFET	$\pi_T = e^{-1925 \left(\frac{1}{T_J + 273} - \frac{1}{298} \right)}$
Diode	$\pi_T = e^{-3091 \left(\frac{1}{T_J + 273} - \frac{1}{298} \right)}$

Table 3. Power loss expressions of components of the boost converter

Component	Power loss
Inductor	$P_D = R_L I_{in}^2$
MOSFET	$P_D = R_{DS(on)} (DI_{in})^2 + \frac{1}{2} V_{out} I_{in} (t_{rise} + t_{fall}) f_s + \frac{1}{2} C_{DS} f_s V_{out}^2$
Diode	$P_D = V_f I_{out} + R_D I_{out}^2 + \frac{1}{2} C_D f_s V_{out}^2$

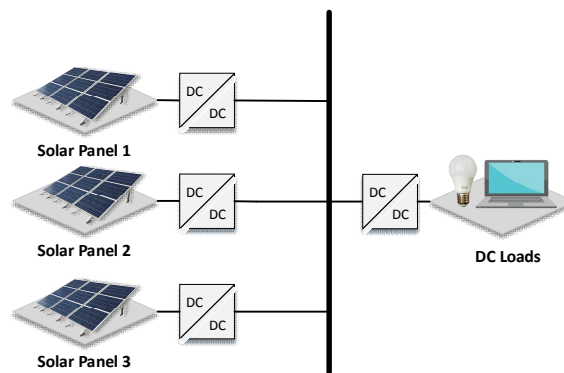


Fig. 2. Solar panels connected to boost converters and a dc bus

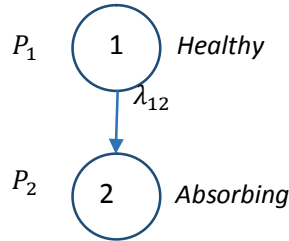


Fig. 3. A Markov-chain model for a dc/dc boost converter connected to a solar panel.

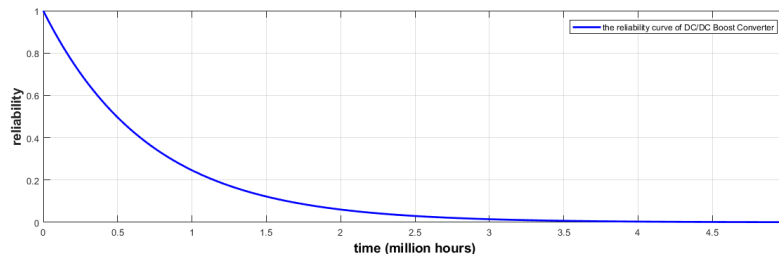


Fig. 4. Reliability curve for the DC/DC Boost Converter

5. CONCLUSIONS

In this paper, a Markovian technique for reliability evaluation of a DC/DC boost converter connected to PV panels has been presented. The reliability of the converter is affected by the failure rate of each of its parts, the temperature factor, and the power dissipation in each part. The overall failure rate of the DC/DC boost converter is used to describe the transition of the converter from its healthy state to its absorbing/failure state. The results show that the reliability of the converter under study is 0.9986 for $t = 1000 \text{ hours}$ and the MTTF is 713247 hours. This result can be used by professionals working in the area of power electronics and their applications for any appropriate maintenance plan or for proposing component replacement/repair before its actual failure so that the downtime of the system can be reduced.

COMPETING INTERESTS

The authors have declared that no competing interests exist.

REFERENCES

1. Xuefeng L, Kaiju L, Weiqiang L, Chaoxu M, Dan W. A brief analysis of distributed generation connected to distribution network, Proc. - 2018 33rd Youth Acad. Annu. Conf. Chinese Assoc. Autom. YAC. 2018;2:795–799. DOI: 10.1109/YAC.2018.8406479.
2. Antonova G, Nardi M, Scott A, Pesin M. Distributed generation and its impact on power grids and microgrids protection, 2012 65th Annu. Conf. Prot. Relay Eng. 2012;152–161. DOI: 10.1109/CPRE.2012.6201229.
3. Bragard M, Soltau N, Thomas S, De Doncker RW. The balance of renewable sources and user demands in grids: Power electronics for modular battery energy storage systems. IEEE Trans. Power Electron. 2010;25(12):3049–3056.
4. Aghdam FH, Hagh MT, Abapour M. Reliability evaluation of two-stage interleaved boost converter interfacing PV panels based on mode of use, 7th Power Electron. Drive Syst. Technol. Conf. PEDSTC. 2016;409–414. DOI: 10.1109/PEDSTC.2016.7556896.
5. Alam MK, Member S, Khan FH, Member S. Reliability analysis and performance degradation of a boost converter. 2014;50(6):3986–3994.
6. Military Handbook: Reliability Prediction of Electronic Equipment. MIL-HDBK-217F. United States Dept. Defense, Arlington, VA, USA; 1991.
7. Dhople SV, Davoudi A, Domínguez-García AD, Chapman PL. A unified approach to

- reliability assessment of multiphase DC-DC converters in photovoltaic energy conversion systems. *IEEE Trans. Power Electron.* 2012;27(2):739–751.
8. Arifujjaman M. Reliability comparison of power electronic converters for grid-connected 1.5kW wind energy conversion system. *Elsevier Renew. Energy.* 2013; 57:348–357,.
 9. De Leon-Aldaco SE, Calleja H, Chan F, JGHR. Effect of the mission profile on the reliability of a power converter aimed at photovoltaic applications— a case study. *IEEE Trans power Electron.* 2013;28(6): 2998–3008
 10. Zhang P, Wang Y, Xiao W, Li W. Reliability evaluation of grid-connected photovoltaic power systems. *IEEE Trans Sustain. Energy.* 2012;3(3):379–389,.
 11. Zargar RHM, Moghaddam MHY. Development of a Markov-Chain-Based solar generation model for smart microgrid energy management system. *IEEE Trans. Sustain. Energy.* 2019;11(2):736–745.
 12. Tushar W, Huang S, Yuen C, Zhang JA, Smith DB. Synthetic generation of solar states for smart grid: A multiple segment Markov chain approach. in *IEEE PES Innovative Smart Grid Technologies, Europe.* 2014;1–6.
 13. Miao S, Ning G, Gu Y, Yan J, Ma B. Markov Chain model for solar farm generation and its application to generation performance evaluation. *J. Clean. Prod.* 2018;186:905–917.
 14. Blin A, Carnino A, Georgin JP, Signoret JP. Use of Markov processes for reliability problems, In *Synthesis and Analysis Methods for Safety and Reliability Studies* Springer, Boston, MA. 1980;269–295.
 15. Papazoglou IA, Gyftopoulos EP. Markov processes for reliability analyses of large systems. *IEEE Trans. Reliab.* 1977;16(3): 232–237.
 16. Britney RR. The reliability of complex systems with dependent subsystem failures: An absorbing Markov chain model. *Technometrics.* 1974;16(2):245–250.
 17. Koutras MV. On a Markov chain approach for the study of reliability structures. *J. Appl. Probab.* 1996;357–367.
 18. Chao MT, Fu JC. The reliability of a large series system under Markov structure. *Adv. Appl. Probab.* 1991;894–908.
 19. Rushdi MAM, Ba-Rukab OM, Rushdi AM. Multi-dimensional recursion relations and mathematical induction techniques: The case of failure frequency of k-out-of-n systems. *J. King Abdulaziz Univ.: Engineering Sciences.* 2016;27(2):15–31.
 20. Trivedi KS. *Probability and statistics with reliability, queueing, and computer science applications.* Englewood Cliffs: NJ:Prentice-hall; 1982.
 21. Reibman A, Trivedi K. Numerical transient analysis of Markov models, *Comput. Oper. Res.* 1998;15(1):19–36.
 22. Shelton CR, Ciardo G. Tutorial on structured continuous-time Markov processes. *J. Artif. Intell. Res.* 2014; 51:725–778.
 23. Wai RJ, Shih LC. Design of voltage tracking control for DC-DC boost converter via total sliding-mode technique, *IEEE Trans. Ind. Electron.* 2011;58(6):2502–2511.
 24. Katore AV, Tech M. Reliability evaluation of multi-level boost converter. 2018;317–322.
 25. Khosroshahi AE, Abapour M, Sabahi M. Reliability evaluation of conventional and interleaved DC-DC boost converters, *IEEE Trans. Power Electron.* 2015;30(10):5821–5828.
 26. Eichhorn T. Boost converter efficiency through accurate calculations. *Power Electron. Technol.* 2008;34(9):30–35.
 27. Littlewood B. A reliability model for systems with Markov structure, *J. R. Stat. Soc. Ser. C (Applied Stat).* 1975; 24(2):172–177,.
 28. Hou K, Jia H, Xu X, Liu Z, Jiang Y. A continuous time Markov chain based sequential analytical approach for composite power system reliability assessment. *IEEE Trans. Power Syst.* 2015;31(1):738–748.
 29. Ye Y, Grossmann IE, Pinto JM, Ramaswamy S. Modeling for reliability optimization of system design and maintenance based on Markov chain theory. *Comput. Chem. Eng.* 2019;124: 381–404.
 30. Bani-Ahmed A, Rashidi M, Nasiri A, Hosseini H. Reliability analysis of a decentralized microgrid control architecture. *IEEE Trans. Smart Grid.* 2018;10(4):3910–3918.
 31. Alvarez-Alvarado MS, Jayaweera D. Bathtub curve as a Markovian process to describe the reliability of repairable components. *IET Gener. Transm. Distrib.* 2018;12(21):5683–5689.

32. Rushdi AM, Bjaili HA. Characterization of time to failure in prognostics: Brief tutorial guide to prognostics professionals. *J. Adv. Math. Comput. Sci.* 2017;25(4):1–15.
33. Klutke GA, Kiessler PC, Wortman MA. A critical look at the bathtub curve. *IEEE Trans. Reliab.* 2003;52(1):125–129.
34. Aarset MV. How to identify a bathtub hazard rate. *IEEE Trans. Reliab.* 1987; 36(1):106–108.
35. Smith RW, Dietrich DL. The bathtub curve: an alternative explanation. in *Proceedings of Annual Reliability and Maintainability Symposium (RAMS) IEEE.* 1994;241–247.
36. Rushdi AM, Alsulami AE. Cost elasticities of reliability and MTTF for k-out-of-n systems. *Journal of Mathematics and Statistics.* 2007;3(3):22-128.
37. Rushdi AM. Partially-redundant systems: Examples, reliability, and life expectancy. *Int. Mag. Adv. Comput. Sci. Telecommun.* 2010;1(1):1–13.
38. Rushdi AM, AK Hassan. An exposition of system reliability analysis with an ecological perspective. *Ecological Indicators.* 2016;63:282-95.
39. Mason SJ. Feedback theory-some properties of signal flow graphs. *Proceedings of the IRE.* 1953;41(9):1144-1156.
40. Mason SJ. Feedback theory: Further properties of signal flow graphs. *Proceedings of the IRE.* 1956;44(7):920-926.
41. Rushdi AM. Utilization of symmetric switching functions in the computation of k-out-of-n system reliability. *Microelectronics and Reliability.* 1986;26(5):973-987.
42. Affandi AM, Rushdi AM. An accurate six-port microstrip reflectometer. In *Microwave and Optoelectronics Conference. Proceedings. SBMO/IEEE MTT-S International, IEEE.* 1995;2:563-568.
43. Golnaraghi F, Kuo BC. *Automatic control systems.* Ninth Edition, Wiley, New York, NY, USA; 2010.
44. Rushdi AA. A mathematical model of DNA replication. *International Magazine on Advances in Computer Science and Telecommunications (IMACST).* 2010; 1(1):23-30.
45. Rushdi AM, Al-Thubaity AO. Efficient computation of the sensitivity of k-out-of-n system reliability. *Microelectronics and Reliability.* 1993;33(13):1963-1979.
46. Rushdi AM, Dehlawi FMA. Optimal computation of k-to-l-out-of-n system reliability. *Microelectronics and Reliability.* 1987;27(5):875-896. Erratum: *ibid.* 1988;28(4):671.
47. Rushdi AM. Threshold systems and their reliability. *Microelectronics and Reliability.* 1990;30(2):299-312.
48. Rushdi AM. Reliability of k-out-of-n Systems. Chapter 5 in K. B. Misra, *New Trends in System Reliability Evaluation, Fundamental Studies in Engineering,* Elsevier Science Publishers, Amsterdam, The Netherlands. 1993;16:185-227.
49. Rushdi AM, Rushdi MA. Switching-algebraic analysis of system reliability, Chapter 6 in M. Ram and P. Davim (Editors), *Advances in Reliability and System Engineering.* Springer International Publishing, Cham, Switzerland. 2017;139-161.
50. Rushdi RA, Rushdi AM, Talmees FA. Novel pedagogical methods for conditional-probability computations in medical disciplines. *Journal of Advances in Medicine and Medical Research.* 2018;25(10):1-15.
51. Rushdi RA, Rushdi AM, Talmees FA. Review of Methods for Conditional-Probability Computations in Medical Disciplines, a Chapter in *Highlights on Medicine and Medical Research,* Book Publishers International, Hooghly, West Bengal, India; 2021.
52. Moler C, Van Loan C. Nineteen dubious ways to compute the exponential of a matrix. *SIAM Review.* 1978;20(4):801-836.
53. Leonard IE. The matrix exponential. *SIAM Review.* 1996;38(3):507-512.
54. Cheng HW, Yau SS. More explicit formulas for the matrix exponential. *Linear Algebra and Its Applications.* 1997;262:131-163.
55. Liz E. Classroom note: A note on the matrix exponential. *SIAM Review.* 1998;40(3):700-702.
56. Moler C, Van Loan C. Nineteen dubious ways to compute the exponential of a matrix, twenty-five years later. *SIAM Review.* 2003;45(1):3-49.
57. Dijkstra EW. Some beautiful arguments using mathematical induction. *Acta Informatica.* 1980;13(1):1-8.
58. Ernest P. Mathematical induction: A pedagogical discussion. *Educational Studies in Mathematics.* 1984;15(2):173-189.

59. Rushdi AM, Ghaleb FA. On self-inverse binary matrices over the binary Galois field. *Journal of Mathematics and Statistics*. 2013;9(3):238-48.
60. Gunderson DS. *Handbook of Mathematical Induction: Theory and applications*. CRC Press; 2014.
61. Rushdi AM, Ghaleb FA. A tutorial exposition of semi-tensor products of matrices with a stress on their representation of boolelean functions. *Journal of King Abdulaziz University: Computing and Information Technology Sciences*. 2016;5(1):3-30.
62. Rushdi MA, Rushdi AM, Zarouan M, Ahmad W. Satisfiability in intuitionistic fuzzy logic with realistic tautology. *Kuwait Journal of Science*. 2018;45(2):15-21.

APPENDIX A

A Two-State Markov Process with Repair

For a general reliability model as shown in Fig A1, the state-transition diagram of the system entails a failure rate λ , a repair rate μ , an up (working) state 1 and a down (failed) state 2. The probability P_1 of the up state is system availability, while the probability P_2 of the down state is system unavailability. The transition-rate matrix of the system $[Q]$ can be obtained from the state-transition diagram in Fig. A1 as follows

$$[Q] = \begin{bmatrix} q_{11} & q_{12} \\ q_{21} & q_{22} \end{bmatrix} = \begin{bmatrix} -\lambda & \lambda \\ \mu & -\mu \end{bmatrix} \quad (A1)$$

We assert that the modern way of drawing the state-transition diagram (highly acclaimed for its simplicity and intuitionistic appeal) deliberately ignores state self-transitions. Therefore, only off-diagonal elements of $[Q]$ are explicitly retrieved from the state-transition diagram in Fig. A1. The element q_{12} stands for the transition rate from state 1 to state 2, and hence it is λ , while the element q_{21} stands for the transition rate from state 2 to state 1, and hence it is μ . The matrix $[Q]$ is a singular matrix of zero determinant, since the sum of elements in every row of it is zero. This property allows us to complete the construction of $[Q]$. Each non-diagonal element in this matrix is expressed as the negative of the sum of other elements in its row.

To get a unique solution of the steady state \vec{P} , we can use the following homogeneous matrix equation

$$[0 \ 0] = [P_1 \ P_2] \begin{bmatrix} -\lambda & \lambda \\ \mu & -\mu \end{bmatrix} \quad (A2)$$

which is equivalent to two linearly-dependent scalar equations, or a single linearly-independent scalar equation. We have to supplement this with a linearly-independent scalar equation, namely, the normalization condition

$$P_1 + P_2 = 1 \quad (A3)$$

The combination of (A2) and (A3) results in the following inhomogeneous matrix equation, which now has a regular matrix

$$[0 \ 1] = [P_1 \ P_2] \begin{bmatrix} -\lambda & 1 \\ \mu & 1 \end{bmatrix} \quad (A4)$$

The matrix equation (A4) is in a form that is very common in operations-research circles. Taking the transpose of both sides of (A4), we obtain a form that is more popular in engineering circles

$$\begin{bmatrix} 0 \\ 1 \end{bmatrix} = \begin{bmatrix} -\lambda & \mu \\ 1 & 1 \end{bmatrix} \begin{bmatrix} P_1 \\ P_2 \end{bmatrix} \quad (A5)$$

We now solve (A5) using determinants according to the celebrated Cramer's Rule, viz.

$$P_1 = \frac{\begin{vmatrix} 0 & \mu \\ 1 & 1 \end{vmatrix}}{\begin{vmatrix} -\lambda & \mu \\ 1 & 1 \end{vmatrix}} = \frac{-\mu}{-(\lambda + \mu)} = \frac{\mu}{\lambda + \mu} \quad (A6a)$$

$$P_2 = \frac{\begin{vmatrix} -\lambda & 0 \\ 1 & 1 \end{vmatrix}}{\begin{vmatrix} -\lambda & \mu \\ 1 & 1 \end{vmatrix}} = \frac{-\lambda}{-(\lambda + \mu)} = \frac{\lambda}{\lambda + \mu} \quad (A6b)$$

The steady state vector $\vec{P} = \begin{bmatrix} \frac{\mu}{\lambda+\mu} \\ \frac{\lambda}{\lambda+\mu} \end{bmatrix}$ so obtained is a well-known result in reliability theory, in particular when the failure rate λ and the repair rate μ are expressed as the reciprocals of the MTTF and the mean time to repair (MTTR).

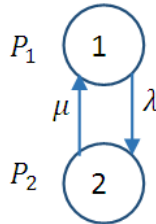


Fig. A1. A Two-State Markov proses with an availability model with a non-zero repair rate

We now handle the transient problem for the Markov process in Fig. A1. The algebraic equation (A2) is replaced by the following ordinary differential equation (ODE)

$$\frac{d}{dt} \vec{P}^T(t) = \vec{P}^T(t)[Q] \tag{A7}$$

This ODE comprises a well-formed initial value problem (IVP), when supplemented with the following initial condition, which assumes that the system is initially good

$$\vec{P}(0) = \begin{bmatrix} P_1(0) \\ P_2(0) \end{bmatrix} = \begin{bmatrix} 1 \\ 0 \end{bmatrix} \tag{A8}$$

We solve this IVP by employing a signal flow graph [19, 39-51] in the transformed (Laplace) domain. We distinguish the time-domain version of a variable from its Laplace-domain version by inserting an overhead bar for the latter version. We identify the time-derivative of a variable with an overhead dot. Hence, we use the symbols $\bar{P}_i(s)$ and $\dot{\bar{P}}_i(s)$ to denote the Laplace transforms of $P_i(t)$ and $\dot{P}_i(t) = \frac{dP_i(t)}{dt}$, respectively. By contrast to the time-domain solution, in which we strive to reduce the number of unknown variables in (A7) from two to one by invoking the normalization condition ($P_1(t) + P_2(t) = 1$), we deliberately double the number of unknown variables in the transformed domain. In fact, we now deal with the four variables $\bar{P}_1(s), \bar{P}_2(s), \dot{\bar{P}}_1(s)$, and $\dot{\bar{P}}_2(s)$, as shown in the SFG of Fig. A2. We construct this SFG by supplying a linear expression of each of these four variables. The expressions for the former two variables are obtained by first expanding (A7) as

$$\begin{bmatrix} \frac{dP_1(t)}{dt} & \frac{dP_2(t)}{dt} \end{bmatrix} = [P_1(t) \quad P_2(t)] \begin{bmatrix} -\lambda & \lambda \\ \mu & -\mu \end{bmatrix}$$

and then transforming it term-wise as

$$\begin{bmatrix} \dot{\bar{P}}_1(s) & \dot{\bar{P}}_2(s) \end{bmatrix} = [\bar{P}_1(s) \quad \bar{P}_2(s)] \begin{bmatrix} -\lambda & \lambda \\ \mu & -\mu \end{bmatrix} \tag{A9}$$

The two latter variables are expressed by first using the following theorem for the transformed derivative

$$\dot{\bar{P}}_i(s) = s\bar{P}_i(s) - P_i(0)$$

and then expressing the transformed variables themselves (for $i = 1, 2$)

$$\bar{P}_i(s) = s^{-1} (\bar{P}_i(s) + P_i(0)) \tag{A10}$$

Equations (A9) and (A10) are used for constructing the SFG in Fig. A2. This SFG has two source nodes, which are specified by the initial conditions (A8). This step reveals an obvious advantage of incorporating the initial conditions from the outset. Since $P_2(0) = 0$, one of the sources of the SFG is annihilated and it disappears.

The SFG is seen to have three loops $L_1 = -\lambda s^{-1}$, $L_2 = -\mu s^{-1}$, $L_3 = \lambda\mu s^{-2}$, where the two loops L_1 and L_2 are not touching. The common denominator to any gain formula is the graph delta given by [43]

$$\begin{aligned} \Delta &= 1 - (L_1 + L_2 + L_3) + L_1L_2 \\ &= 1 + \lambda s^{-1} + \mu s^{-1} - \lambda\mu s^{-2} + (-\lambda s^{-1})(-\mu s^{-1}) \\ &= 1 + (\lambda + \mu) s^{-1} \end{aligned}$$

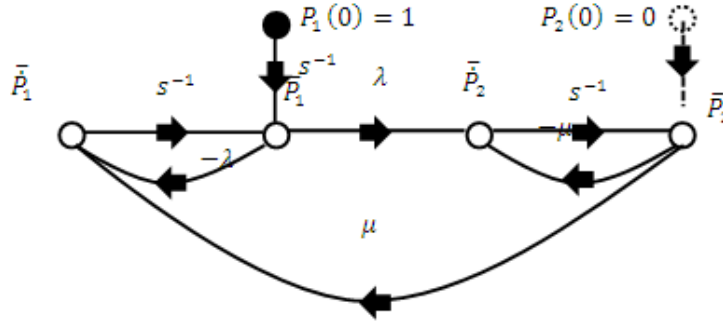


Fig. A2. A signal flow graph for analyzing the Markov process in Fig. A1 in the Laplace (s) domain

Therefore, the transformed state probabilities are obtained via Mason gain formula [43] as

$$\bar{P}_1(s) = \frac{s^{-1}[1-L_2]}{\Delta} = \frac{s^{-1}[1+\mu s^{-1}]}{1+(\lambda+\mu)s^{-1}} = \frac{s+\mu}{s[s+(\lambda+\mu)]}$$

$$\bar{P}_2(s) = \frac{\lambda s^{-2}}{\Delta} = \frac{\lambda}{s[s+(\lambda+\mu)]}$$

The sum of the two state probabilities are

$$\bar{P}_1(s) + \bar{P}_2(s) = \frac{s + \mu + \lambda}{s[s + (\lambda + \mu)]} = \frac{1}{s}$$

This is a good check, since it verifies the normalization condition: $P_1(t) + P_2(t) = 1$ for $t \geq 0$.

Now, we express the first transformed probability as a sum of two partial fractions

$$\bar{P}_1(s) = \frac{A}{s} + \frac{B}{s + (\lambda + \mu)}$$

$$A = \left. \frac{s + \mu}{s + (\lambda + \mu)} \right|_{s=0} = \frac{\mu}{\lambda + \mu}$$

$$B = \left. \frac{s + \mu}{s} \right|_{s=-(\lambda+\mu)} = \frac{-\lambda}{-(\lambda + \mu)} = \frac{\lambda}{\lambda + \mu}$$

$$\bar{P}_1(s) = \frac{1}{\lambda + \mu} \left[\frac{\mu}{s} + \frac{\lambda}{s + (\lambda + \mu)} \right]$$

For $t \geq 0$, we obtain

$$P_1(t) = \frac{1}{\lambda + \mu} [\mu + \lambda e^{-(\lambda + \mu)t}]$$

and we check that the steady-state value is as obtained before

$$\lim_{t \rightarrow \infty} P_1(t) = \frac{\mu}{\lambda + \mu}$$

We now repeat the previous steps for the second transformed probability, namely

$$\bar{P}_2(s) = \frac{C}{s} + \frac{D}{s + (\lambda + \mu)}$$

$$C = \frac{\lambda}{s + (\lambda + \mu)} \Big|_{s=0} = \frac{\lambda}{\lambda + \mu}$$

$$D = \frac{\lambda}{s} \Big|_{s=-(\lambda + \mu)} = -\frac{\lambda}{\lambda + \mu}$$

$$\bar{P}_2(s) = \frac{1}{\lambda + \mu} \left[\frac{\lambda}{s} - \frac{\lambda}{s + (\lambda + \mu)} \right]$$

For $t \geq 0$, we obtain

$$P_2(t) = \frac{1}{\lambda + \mu} [\lambda - \lambda e^{-(\lambda + \mu)t}]$$

and again we check that the steady-state value is as obtained before

$$\lim_{t \rightarrow \infty} P_2(t) = \frac{\lambda}{\lambda + \mu}$$

We can also recover (9) when there is no repair, and we can as well check the normalization condition in the time domain

$$P_1(t) + P_2(t) = 1 \text{ for } t \geq 0$$

We now construct a time-domain solution by deriving the exponential [52-56] of the transition-rate matrix. First, we obtain the square of this matrix as

$$\begin{aligned} [Q]^2 &= \begin{bmatrix} -\lambda & \lambda \\ \mu & -\mu \end{bmatrix} \begin{bmatrix} -\lambda & \lambda \\ \mu & -\mu \end{bmatrix} = \begin{bmatrix} \lambda^2 + \lambda\mu & -\lambda^2 - \lambda\mu \\ -\lambda\mu - \mu^2 & \lambda\mu + \mu^2 \end{bmatrix} \\ &= -(\lambda + \mu) \begin{bmatrix} -\lambda & \lambda \\ \mu & -\mu \end{bmatrix} = -(\lambda + \mu)[Q] \end{aligned}$$

Hence, we can utilize mathematical induction [19. 57-62] to obtain the k^{th} power of this matrix as

$$[Q]^k = (-1)^{k-1} (\lambda + \mu)^{k-1} [Q], \quad k \geq 1$$

Now, the exponential of the matrix is obtained via the uniformly-convergent infinite sum

$$\begin{aligned} e^{[Q]t} &= \sum_{k=0}^{\infty} \frac{[Q]^k t^k}{k!} = [I] + \frac{-1}{\lambda + \mu} \sum_{k=1}^{\infty} \frac{(-(\lambda + \mu)t)^k}{k!} [Q] \\ &= [I] - \frac{e^{-(\lambda + \mu)t}}{\lambda + \mu} [Q] + \frac{1}{\lambda + \mu} [Q] \\ &= \frac{1}{\lambda + \mu} \begin{bmatrix} \mu & \lambda \\ \mu & \lambda \end{bmatrix} - \frac{1}{\lambda + \mu} e^{-(\lambda + \mu)t} [Q] \end{aligned}$$

and finally the probability vector is obtained as

$$\begin{aligned} \vec{p}^T(t) &= \vec{p}^T(0)e^{[Q]t} = [1 \quad 0]e^{[Q]t} \\ &= \frac{1}{\lambda + \mu} [\mu \quad \lambda] - \frac{1}{\lambda + \mu} e^{-(\lambda + \mu)t} [-\lambda \quad \lambda] = \\ &= \frac{1}{\lambda + \mu} [\mu + \lambda e^{-(\lambda + \mu)t} \quad \lambda - \lambda e^{-(\lambda + \mu)t}] \end{aligned}$$

in agreement with our previous results.

© 2021 Muktiadji and Rushdi; This is an Open Access article distributed under the terms of the Creative Commons Attribution License (<http://creativecommons.org/licenses/by/4.0>), which permits unrestricted use, distribution, and reproduction in any medium, provided the original work is properly cited.

Peer-review history:
 The peer review history for this paper can be accessed here:
<http://www.sdiarticle4.com/review-history/64839>